

THE ULTRAVIOLET CALIBRATION OF THE HUBBLE SPACE TELESCOPE. I. SECONDARY STANDARDS OF ABSOLUTE ULTRAVIOLET FLUX AND THE RECALIBRATION OF *IUE*

RALPH C. BOHLIN

Space Telescope Science Institute

Received 1986 January 10; accepted 1986 February 21

ABSTRACT

Now that the *IUE* flux scale has been generally accepted and verified to the quoted errors of $\pm 10\%$, spectral energy distributions of *IUE* standards are needed. The five UV standards, HD 60753, BD +75°325, HD 93521, BD +33°2642, and BD +28°4211, were well observed in the original calibration epoch of the *IUE* observatory and have been monitored for UV variability since the *IUE* launch in 1978. Only observations from the first year of *IUE* were used to define the standard fluxes, in order to avoid the problem of the gradual degradation of the *IUE* sensitivity. These five standard stars are the basis for evaluating later epoch *IUE* sensitivities and for calibrating the UV-sensitive instruments on the Hubble Space Telescope.

During the process of preparing these early-epoch *IUE* fluxes for publication, an error in the original *IUE* calibration of Bohlin and Holm for the low-dispersion mode was discovered and corrected. The early *IUE* calibration work used an average of spectra from both the large and the small entrance apertures with the assumption that their relative response was gray over the entire spectral range. Since recent studies have shown that the small-aperture sensitivity drops by as much as 30% at 3200 Å in the LWR camera, an error as large as 10% at 3200 Å is present in the *IUE* calibration when applied to a large-aperture spectrum.

The corrected *IUE* fluxes for BD +28°4211 and BD +33°2642 are compared to ground-based measurements of stellar flux below the Balmer limit by Stone. Using a simple model to extrapolate the *IUE* flux distribution to wavelengths longward of 3200 Å, the mean difference between *IUE* and the Stone fluxes is less than 2% for BD +28°4211 and $\sim 1\%$ for BD +33°2642.

The corrected *IUE* absolute calibrations for the SWP and LWR cameras in the initial epoch are presented.

Subject headings: spectrophotometry — ultraviolet: spectra

I. INTRODUCTION

The original absolute sensitivity calibration of the low-dispersion mode of the *IUE* SWP and LWR cameras was based on η UMa and several measurements of UV fluxes by earlier experiments. The relation of the *IUE* flux scale to these other instruments is shown graphically in Bohlin *et al.* (1980) and in tabular form in Bohlin and Holm (1984). *IUE* absolute fluxes are based on the 1980 May calibration of Bohlin and Holm (1980), which also appears in Holm *et al.* (1982). The preliminary calibration of Bohlin *et al.* (1980) was superseded by the 1980 May calibration, which is the only sensitivity calibration for SWP and LWR that has ever been used in routine *IUE* science data processing.

The derivation of fluxes from the *IUE* data is complicated by the observed sensitivity losses of up to $2.5\% \text{ yr}^{-1}$

(Sonneborn 1984). However, mean fluxes of stars that were well observed in both SWP and LWR throughout the initial epoch from 1978 April to 1979 April are unaffected by sensitivity changes to an accuracy of better than 1%. Observations with no trailing of the five stars that satisfy these criteria are summarized in Table 1. Because of the high statistical weight of the numerous observations of the five program stars in the first year of *IUE*, these stars are used as the practical definition of the *IUE* flux scale. The study by Sonneborn (1984) of the UV fluxes of the program stars over the lifetime of the *IUE* has revealed no evidence for stellar variability on long time scales, since the trends are the same to an accuracy of 1%–2% for all five stars studied. On shorter time scales, the upper limit on variability is comparable to the scatter of $\sim 3\%$ in the broad bands studied by Sonneborn.

TABLE 1
OBSERVATIONS OF PROGRAM STARS BETWEEN 1978 APRIL AND 1979 APRIL

STAR	R.A. (1950)	DECL. (1950)	SP.	V	B – V	REFERENCE	NUMBER OF SWP SPECTRA ^a		NUMBER OF LWR SPECTRA ^a			
							P	S	P	S	$\sigma(\text{LWR})^b$	
HD 60753	7 ^h 32 ^m 08 ^s .1	–50°28'29"	B3 IV	6.69	–0.09	1	6	5	3.9%	5	4	6.1%
BD +75°325	8 04 43.2	+75 06 48	O5p	9.54	–0.37	2, 3	7	6	4.1	7	6	6.2
HD 93521	10 45 33.6	+37 50 04	O9 Vp	7.04	–0.28	4	15	13	4.9	13	13	6.9
BD +33°2642	15 50 01.9	+33 05 28	B2 IV	10.83	–0.16	3	8	4	5.1	7	4	7.4
BD +28°4211	21 48 57.4	+28 37 34	Op	10.54	–0.34	2, 3	12	12	5.4	7	6	6.7

^a P, point source in large aperture; S, source in small aperture.

^b Mean standard deviation, 1σ , of all 5 Å bins of Table 2.

REFERENCES.—(1) Jamar *et al.* 1976. (2) Goy 1973. (3) Jaschek *et al.* 1972. (4) Guetter 1974.

II. DATA REDUCTION

a) Correction of Systematic Errors

The *IUE* spectra were all extracted by the image processing system that was in routine use between 1978 July and 1979 May. Certain errors were present in those early extractions, as reviewed by Turnrose, Thompson, and Gass (1984). The following corrections were made to the extracted spectra:

1. All wavelength assignments were corrected to the mean small aperture dispersion constants of Turnrose, Bohlin, and Harvel (1979) with the displacements for the large aperture given by Turnrose *et al.* (1979). The correction procedure is specified by Harvel, Turnrose, and Bohlin (1979).

2. The correction algorithm that was adopted by the three *IUE* agencies was applied to remedy the original error in the intensity transfer function (ITF) for the SWP camera (Holm *et al.* 1982). Any data that might have been processed using an even earlier, preliminary ITF was reprocessed to this uniform, known basis. The purpose of the ITF is to linearize the *IUE* response in converting data numbers (DN) to flux numbers (FN) and to reduce the spectra to a uniform flat field.

3. All spectra were corrected to the mean camera head temperature of 8°C for SWP and 12°C for LWR by using the changes in camera sensitivity with temperature of $-0.5\% \text{ }^{\circ}\text{C}^{-1}$ for SWP and $-1.1\% \text{ }^{\circ}\text{C}^{-1}$ for LWR (Schiffer 1982). Mean temperatures for all the spectra discussed here are within 0.5°C of the overall means, so that the total effect of the temperature correction on the fluxes in Table 2 is less than 0.5%

4. The large aperture exposure times were corrected for the high voltage rise time of 0.12 s (Schiffer 1980) after truncating the specified exposure time to an integral multiple of 0.4096 s. Corrections to the small-aperture exposure times are irrelevant, since the small-aperture data are normalized to the large aperture. The primary effect of the 0.12 s correction is an increase in the HD 93521 fluxes of 4% with respect to the faintest stars. Bohlin and Holm did not make a high voltage rise time correction in deriving the 1980 May calibration, since the effect was not appreciated at the time. If 0.12 s had been subtracted from the exposure times originally, the inverse sensitivity of 1980 May and all fluxes based on *IUE* scale would be only 1% lower.

5. The small-aperture spectra were corrected to be of the same relative response as the large-aperture by using the smooth correction factors discussed in § III. The data specified in Table 1 in conjunction with a comparable set of *IUE* observations taken in 1981 were used to define the small to large aperture ratios (S/L), which are normalized to an average value of unity. The smoothed S/L corrections are typically within 5% of unity for the SWP camera and for LWR below 3100 Å, but S/L falls to 0.7 at 3200 Å. The S/L ratios for the 1978–1979 data and for the 1981 data differ by less than the rms scatter of the two separate determinations, indicating that S/L is largely time-independent. Statistically significant structure at the few-percent level is present in the unsmoothed S/L with a correlation length of several resolution elements, despite the fact that the *IUE* production data processing is designed to reduce all spectra to a common flat field. The systematic and largest deviations of S/L from unity longward of 3100 Å may be attributable to a flat-field correction at this extreme of the CsTe cathode sensitivity that differs from the flat field in the ITF correction, which is based on 2537 Å light from a mercury penray lamp. Possible explanations for the fine structure in the unsmoothed S/L include: (1) the noise in the ITF is systemati-

cally impressed on each reduced spectrum and becomes evident in the high signal-to-noise results of this work, and (2) the cameras had not stabilized to the normal guest observer mode when the ITF was obtained in the early commissioning period of *IUE*.

b) Procedures

In addition to the correction of individual spectra for the above effects, the steps outlined below were followed to create the mean spectrum for each star in Table 2.

1. After the SWP ITF correction, the net spectrum was computed from the gross by subtracting a background that had a 31 point median filter applied and was smoothed twice by averaging over 15 points. The LWR net was created by the production processing system.

2. The effective exposure times for small-aperture spectra were computed by normalizing to the mean of the large-aperture spectra in the interval 1600–1725 Å for SWP and 2500–2700 Å for LWR.

3. The sum of the calibrated net spectra $\sum A$ were accumulated in 5 Å bins, while the sum of the exposure times $\sum t$, or effective exposure times for the small aperture, were accumulated for the same bins.

4. If any point was flagged as a reseau or other contaminant, no contribution was made to either $\sum A$ or $\sum t$. The effect of this procedure is that the net flux at positions of large-aperture reseaux is defined entirely by small-aperture data, and vice versa. The reduced number of spectra used to define the standard flux in Table 2 is reflected in the reduced number of points under NO. in the table.

5. The rms scatter of all spectra within each bin is listed in percent under SIGMA in Table 2, while the average scatter is summarized in Table 1. The rms scatter is only 5% for bins at wavelengths as short as 1200 Å. However, the scatter increases dramatically in the region of the strong Ly α line. The causes for this increased uncertainty are: (1) the rapid change in flux over the 5 Å bins makes the average flux in any spectrum very sensitive to small wavelength errors, and (2) the lower signal in the line results in larger statistical uncertainty. In addition, variable geocoronal Ly α may contribute, especially for the faintest star, BD +33°2642, where the rms scatter rises to 39% at 1215 Å.

6. The absolute flux is $F = \sum A / \sum t$. The units of this FLUX in Table 2 are $\text{ergs cm}^{-2} \text{ s}^{-1} \text{ \AA}^{-1}$. The wavelengths (LAMBDA) are in Å.

c) Quality Control

The following were considered in an effort to have the highest quality set of uniform data for the *IUE* standards.

1. Spectra with data near saturation were avoided, since exposure times were calculated to keep the response below the level where errors could occur due to truncations or extrapolations in the ITF. The process of extrapolation does not introduce additional errors (Holm 1981), but extrapolated points are often near saturation, where nonlinearity errors are worse.

2. All spectra with pronounced microphonics noise were excluded.

3. All images with telemetry dropouts were excluded.

d) Uncorrected Errors

Certain known errors that have not been corrected are still associated with the spectra of the UV flux standards.

TABLE 2A
HD 60753

LAMBDA	FLUX	SIGMA NO.									
SWP											
1155	9.41E-11	6.1 11	1360	9.78E-11	3.2 11	1565	6.63E-11	2.4 11	1770	5.90E-11	4.7 11
1160	1.01E-10	5.6 11	1365	9.34E-11	3.5 11	1570	6.82E-11	5.9 11	1775	5.74E-11	4.4 11
1165	9.95E-11	6.2 11	1370	9.45E-11	3.1 11	1575	6.84E-11	6.2 7	1780	5.89E-11	2.7 5
1170	9.33E-11	5.4 11	1375	9.24E-11	2.8 11	1580	6.66E-11	3.3 6	1785	5.87E-11	1.5 5
1175	7.45E-11	3.7 11	1380	9.10E-11	3.8 11	1585	7.03E-11	3.5 6	1790	5.82E-11	2.9 5
1180	8.98E-11	7.0 8	1385	9.20E-11	1.8 11	1590	6.97E-11	3.1 6	1795	6.16E-11	2.1 5
1185	9.79E-11	3.3 5	1390	8.64E-11	2.9 11	1595	6.79E-11	4.5 6	1800	6.12E-11	3.3 8
1190	8.81E-11	4.9 5	1395	7.96E-11	3.5 11	1600	6.64E-11	3.4 11	1805	5.97E-11	2.8 11
1195	7.43E-11	4.4 5	1400	8.47E-11	3.2 11	1605	6.40E-11	4.3 11	1810	5.77E-11	2.6 11
1200	5.95E-11	5.5 5	1405	8.39E-11	1.9 11	1610	6.23E-11	2.3 11	1815	5.75E-11	2.6 11
1205	2.76E-11	9.2 11	1410	8.40E-11	2.6 11	1615	6.37E-11	3.8 11	1820	5.73E-11	3.4 11
1210	9.46E-12	11.4 11	1415	8.24E-11	3.8 11	1620	6.37E-11	3.9 11	1825	5.70E-11	2.6 11
1215	4.67E-12	24.7 11	1420	8.42E-11	2.7 11	1625	6.25E-11	3.9 11	1830	5.60E-11	2.2 11
1220	1.70E-11	20.2 11	1425	8.70E-11	3.0 11	1630	6.29E-11	2.9 11	1835	5.49E-11	3.0 11
1225	4.70E-11	10.1 11	1430	8.85E-11	2.9 11	1635	6.21E-11	4.0 11	1840	5.30E-11	3.2 11
1230	7.17E-11	7.5 11	1435	8.57E-11	3.1 11	1640	6.37E-11	3.0 11	1845	5.14E-11	3.9 11
1235	9.10E-11	6.1 11	1440	8.86E-11	4.9 11	1645	6.50E-11	3.6 11	1850	4.94E-11	4.4 11
1240	1.06E-10	3.4 11	1445	9.02E-11	2.7 10	1650	6.18E-11	3.9 6	1855	4.60E-11	3.8 11
1245	1.07E-10	3.1 11	1450	9.01E-11	1.9 6	1655	6.20E-11	2.9 5	1860	4.76E-11	3.6 11
1250	1.04E-10	3.2 11	1455	8.86E-11	2.1 6	1660	6.02E-11	5.3 5	1865	4.86E-11	3.8 11
1255	1.08E-10	4.2 11	1460	8.74E-11	2.8 6	1665	6.12E-11	2.7 7	1870	5.17E-11	2.2 11
1260	9.51E-11	4.4 11	1465	8.66E-11	3.0 10	1670	6.22E-11	2.3 11	1875	5.17E-11	2.6 11
1265	9.70E-11	1.8 11	1470	8.54E-11	3.8 11	1675	5.91E-11	3.5 11	1880	4.96E-11	3.6 11
1270	1.11E-10	2.8 11	1475	8.45E-11	2.7 11	1680	6.28E-11	4.7 11	1885	4.65E-11	2.7 11
1275	1.08E-10	3.1 11	1480	8.76E-11	2.8 11	1685	6.37E-11	4.9 11	1890	4.50E-11	3.1 11
1280	1.12E-10	4.4 11	1485	8.41E-11	3.4 11	1690	6.46E-11	4.8 11	1895	4.47E-11	3.1 11
1285	1.11E-10	4.0 11	1490	8.80E-11	3.2 11	1695	6.35E-11	3.4 11	1900	4.56E-11	3.7 11
1290	1.02E-10	3.2 11	1495	8.54E-11	1.9 11	1700	6.25E-11	4.5 11	1905	4.48E-11	3.3 11
1295	8.63E-11	4.8 11	1500	8.17E-11	2.7 11	1705	6.04E-11	5.2 11	1910	4.47E-11	2.3 11
1300	7.29E-11	1.9 11	1505	8.01E-11	2.5 11	1710	5.77E-11	3.9 11	1915	4.36E-11	3.7 7
1305	7.39E-11	3.4 11	1510	7.67E-11	3.9 11	1715	5.65E-11	3.4 11	1920	4.28E-11	2.0 5
1310	8.99E-11	3.0 11	1515	7.44E-11	5.2 11	1720	5.51E-11	2.4 11	1925	4.21E-11	2.4 5
1315	1.12E-10	4.6 11	1520	7.69E-11	5.9 11	1725	5.44E-11	3.9 11	1930	4.19E-11	1.8 5
1320	1.12E-10	2.1 10	1525	7.55E-11	5.4 11	1730	6.08E-11	4.5 11	1935	4.36E-11	2.0 7
1325	1.04E-10	2.4 11	1530	7.16E-11	6.6 11	1735	6.09E-11	3.4 11	1940	4.39E-11	2.9 11
1330	9.59E-11	4.0 11	1535	7.03E-11	2.4 11	1740	6.05E-11	3.5 11	1945	4.54E-11	2.0 11
1335	8.04E-11	3.3 11	1540	6.90E-11	3.4 11	1745	6.04E-11	3.9 11	1950	4.44E-11	3.1 11
1340	1.00E-10	3.5 11	1545	7.00E-11	4.3 11	1750	5.86E-11	3.5 11	1955	4.35E-11	3.1 11
1345	1.02E-10	6.1 11	1550	6.68E-11	2.6 11	1755	6.04E-11	4.7 11	1960	4.38E-11	3.0 11
1350	1.00E-10	4.5 11	1555	7.10E-11	6.4 11	1760	5.94E-11	4.0 11	1965	4.42E-11	3.8 11
1355	1.01E-10	3.2 11	1560	6.80E-11	3.2 11	1765	5.90E-11	4.1 11	1970	4.56E-11	4.3 11
LAMBDA	FLUX	SIGMA NO.									
LWR											
1900	4.39E-11	14.8 9	2160	3.58E-11	4.1 5	2420	3.14E-11	4.8 9	2680	2.93E-11	3.2 6
1905	4.63E-11	11.2 9	2165	3.37E-11	4.0 5	2425	3.16E-11	4.6 9	2685	2.95E-11	5.3 6
1910	4.81E-11	12.8 9	2170	3.65E-11	7.6 5	2430	3.26E-11	4.7 9	2690	2.99E-11	6.0 6
1915	4.30E-11	14.9 9	2175	3.73E-11	8.9 5	2435	3.15E-11	4.6 9	2695	2.76E-11	2.7 6
1920	4.32E-11	11.0 9	2180	3.53E-11	9.2 5	2440	3.14E-11	5.8 9	2700	2.67E-11	4.0 6
1925	4.65E-11	8.0 9	2185	3.78E-11	4.3 5	2445	3.33E-11	4.1 9	2705	2.86E-11	3.2 6
1930	5.04E-11	11.6 9	2190	4.27E-11	9.2 6	2450	3.28E-11	3.6 9	2710	2.75E-11	4.1 9
1935	4.83E-11	7.9 9	2195	4.09E-11	20.3 9	2455	3.26E-11	8.1 9	2715	2.71E-11	3.4 9
1940	4.73E-11	5.7 9	2200	3.65E-11	8.0 9	2460	3.23E-11	5.9 9	2720	2.67E-11	3.4 9
1945	4.62E-11	9.7 9	2205	3.30E-11	5.9 9	2465	3.22E-11	3.4 9	2725	2.65E-11	3.2 9
1950	4.58E-11	8.7 9	2210	3.38E-11	9.4 9	2470	3.08E-11	3.7 9	2730	2.69E-11	4.6 9
1955	4.34E-11	6.9 6	2215	3.40E-11	4.7 9	2475	2.96E-11	6.2 9	2735	2.69E-11	4.9 9
1960	4.18E-11	5.2 6	2220	3.32E-11	6.6 9	2480	3.05E-11	5.5 9	2740	2.62E-11	4.6 9
1965	3.96E-11	6.7 6	2225	3.41E-11	9.1 9	2485	3.09E-11	8.6 9	2745	2.53E-11	5.0 9
1970	4.29E-11	3.8 6	2230	3.38E-11	6.8 9	2490	2.98E-11	5.5 9	2750	2.54E-11	2.9 9
1975	4.84E-11	5.5 6	2235	3.20E-11	5.9 9	2495	2.92E-11	7.5 9	2755	2.60E-11	4.3 9
1980	4.71E-11	7.8 9	2240	3.14E-11	6.0 9	2500	3.27E-11	5.0 9	2760	2.48E-11	3.6 9
1985	4.56E-11	9.7 9	2245	3.23E-11	6.5 9	2505	3.19E-11	3.3 9	2765	2.53E-11	5.0 9
1990	4.47E-11	4.7 9	2250	3.28E-11	8.8 9	2510	3.03E-11	4.5 9	2770	2.54E-11	5.0 9
1995	4.40E-11	7.3 9	2255	3.48E-11	7.0 9	2515	2.97E-11	3.6 9	2775	2.58E-11	3.4 9
2000	4.25E-11	6.0 9	2260	3.56E-11	5.8 9	2520	2.94E-11	3.7 9	2780	2.63E-11	3.2 8
2005	4.40E-11	6.5 9	2265	3.44E-11	4.8 9	2525	2.89E-11	4.1 9	2785	2.56E-11	3.4 8
2010	4.48E-11	4.4 9	2270	3.40E-11	6.3 9	2530	3.00E-11	2.7 9	2790	2.68E-11	6.4 8
2015	4.33E-11	4.6 9	2275	3.53E-11	6.5 9	2535	3.00E-11	3.9 9	2795	2.43E-11	7.1 9
2020	4.47E-11	5.6 9	2280	3.64E-11	3.6 9	2540	2.93E-11	3.5 9	2800	2.31E-11	3.6 8
2025	4.57E-11	5.7 9	2285	3.43E-11	4.3 9	2545	2.97E-11	5.0 9	2805	2.46E-11	3.6 8
2030	4.42E-11	4.1 9	2290	3.40E-11	3.8 9	2550	3.08E-11	4.9 9	2810	2.40E-11	4.2 9
2035	4.26E-11	3.7 9	2295	3.32E-11	5.2 9	2555	2.97E-11	5.0 9	2815	2.61E-11	5.0 9
2040	4.16E-11	4.7 9	2300	3.32E-11	7.3 9	2560	2.89E-11	4.3 9	2820	2.64E-11	3.4 9
2045	4.33E-11	5.8 9	2305	3.51E-11	6.7 9	2565	3.03E-11	2.1 7	2825	2.50E-11	5.5 9
2050	4.17E-11	7.5 8	2310	3.49E-11	7.3 9	2570	3.04E-11	1.9 4	2830	2.38E-11	4.4 9
2055	3.96E-11	7.0 7	2315	3.33E-11	3.9 9	2575	2.97E-11	3.2 4	2835	2.40E-11	2.4 9
2060	4.13E-11	5.0 7	2320	3.39E-11	6.7 9	2580	2.98E-11	2.7 9	2840	2.38E-11	3.3 9
2065	4.19E-11	5.1 7	2325	3.55E-11	4.6 9	2585	2.99E-11	4.0 4	2845	2.46E-11	4.9 9
2070	4.01E-11	4.9 7	2330	3.57E-11	5.6 9	2590	2.82E-11	5.4 9	2850	2.50E-11	4.2 9
2075	4.17E-11	4.7 7	2335	3.35E-11	6.5 9	2595	2.70E-11	4.3 4	2855	2.41E-11	2.8 9
2080	4.29E-11	5.1 9	2340	3.26E-11	3.4 9	2600	2.83E-11	2.4 4	2860	2.51E-11	4.1 9
2085	4.07E-11	5.4 9	2345	3.30E-11	4.8 9	2605	2.95E-11	4.5 7	2865	2.49E-11	4.1

TABLE 2B
BD +75°325

LAMBDA	FLUX	SIGMA NO.									
SWP											
1155	1.02E-10	8.0 13	1360	5.48E-11	3.9 13	1565	3.71E-11	3.0 13	1770	2.80E-11	4.7 13
1160	1.04E-10	6.3 13	1365	5.53E-11	3.1 13	1570	3.65E-11	3.5 13	1775	2.80E-11	3.1 13
1165	9.91E-11	6.0 13	1370	5.50E-11	3.8 13	1575	3.77E-11	3.1 12	1780	2.77E-11	4.0 6
1170	9.31E-11	4.7 13	1375	5.31E-11	3.5 13	1580	3.70E-11	3.7 7	1785	2.72E-11	2.8 6
1175	8.91E-11	6.8 13	1380	5.64E-11	3.5 13	1585	3.64E-11	3.6 7	1790	2.66E-11	3.4 6
1180	9.28E-11	5.8 10	1385	5.38E-11	6.4 13	1590	3.61E-11	3.0 7	1795	2.72E-11	4.0 6
1185	9.18E-11	4.4 6	1390	5.30E-11	3.1 13	1595	3.49E-11	4.6 7	1800	2.64E-11	3.5 11
1190	8.80E-11	3.1 6	1395	5.20E-11	4.3 13	1600	3.49E-11	5.1 13	1805	2.60E-11	4.3 13
1195	7.80E-11	3.0 6	1400	5.25E-11	4.6 13	1605	3.34E-11	4.1 13	1810	2.60E-11	3.7 13
1200	7.65E-11	4.1 6	1405	4.96E-11	4.0 13	1610	3.14E-11	4.1 13	1815	2.63E-11	3.4 13
1205	8.25E-11	5.1 13	1410	5.02E-11	2.9 13	1615	3.13E-11	3.1 13	1820	2.68E-11	5.0 13
1210	6.97E-11	6.4 13	1415	5.14E-11	3.8 13	1620	3.05E-11	3.7 13	1825	2.60E-11	2.4 13
1215	5.05E-11	10.2 13	1420	4.98E-11	4.2 13	1625	3.05E-11	3.5 13	1830	2.59E-11	2.7 13
1220	7.02E-11	10.3 13	1425	5.07E-11	3.5 13	1630	3.02E-11	3.8 13	1835	2.53E-11	3.2 13
1225	7.98E-11	5.5 13	1430	4.97E-11	2.8 13	1635	2.87E-11	4.4 13	1840	2.44E-11	3.5 13
1230	7.75E-11	4.7 13	1435	4.99E-11	4.4 13	1640	2.66E-11	4.4 13	1845	2.48E-11	4.4 13
1235	7.04E-11	4.4 13	1440	4.78E-11	5.2 13	1645	2.93E-11	4.0 13	1850	2.40E-11	5.2 13
1240	6.28E-11	5.6 13	1445	4.67E-11	3.7 13	1650	3.05E-11	3.2 9	1855	2.36E-11	5.0 13
1245	6.96E-11	5.4 13	1450	4.59E-11	4.3 7	1655	2.98E-11	3.0 6	1860	2.42E-11	5.6 13
1250	6.98E-11	3.9 13	1455	4.58E-11	2.4 7	1660	2.92E-11	2.4 6	1865	2.43E-11	4.2 13
1255	7.06E-11	3.6 13	1460	4.72E-11	2.3 7	1665	3.00E-11	2.5 8	1870	2.45E-11	4.0 13
1260	7.20E-11	3.0 13	1465	4.79E-11	3.2 10	1670	2.97E-11	2.7 13	1875	2.39E-11	3.0 13
1265	7.41E-11	4.6 13	1470	4.71E-11	5.2 13	1675	2.96E-11	2.6 13	1880	2.34E-11	2.7 13
1270	7.32E-11	3.0 13	1475	4.68E-11	4.6 13	1680	3.03E-11	2.8 13	1885	2.23E-11	4.8 13
1275	7.60E-11	3.1 13	1480	4.79E-11	4.2 13	1685	3.05E-11	6.0 13	1890	2.29E-11	3.7 13
1280	7.48E-11	3.5 13	1485	4.70E-11	5.7 13	1690	3.00E-11	6.0 13	1895	2.30E-11	3.0 13
1285	7.30E-11	3.3 13	1490	4.76E-11	3.4 13	1695	3.02E-11	2.0 13	1900	2.24E-11	4.6 13
1290	7.62E-11	3.7 13	1495	4.73E-11	3.9 13	1700	2.93E-11	2.5 13	1905	2.17E-11	6.0 13
1295	7.69E-11	3.0 13	1500	4.50E-11	5.0 13	1705	2.97E-11	4.2 13	1910	2.15E-11	5.2 13
1300	7.16E-11	3.9 13	1505	4.49E-11	2.9 13	1710	2.92E-11	3.7 13	1915	2.16E-11	4.8 9
1305	6.85E-11	4.0 13	1510	4.55E-11	5.0 13	1715	2.73E-11	3.6 13	1920	2.07E-11	3.9 6
1310	6.68E-11	3.7 13	1515	4.47E-11	3.5 13	1720	2.58E-11	3.8 13	1925	2.11E-11	4.3 6
1315	6.53E-11	3.8 13	1520	4.55E-11	2.9 13	1725	2.74E-11	4.2 13	1930	2.12E-11	6.4 6
1320	6.56E-11	4.3 13	1525	4.46E-11	4.3 13	1730	2.85E-11	3.9 13	1935	2.09E-11	5.6 9
1325	6.81E-11	2.5 13	1530	4.22E-11	4.7 13	1735	2.89E-11	5.3 13	1940	2.09E-11	2.9 13
1330	6.49E-11	3.7 13	1535	4.21E-11	4.8 13	1740	2.85E-11	4.9 13	1945	2.09E-11	2.8 13
1335	6.24E-11	3.1 13	1540	4.26E-11	4.3 13	1745	2.89E-11	3.6 13	1950	2.10E-11	4.3 13
1340	6.32E-11	3.6 13	1545	4.05E-11	4.7 13	1750	2.80E-11	3.8 13	1955	2.10E-11	4.8 13
1345	6.19E-11	5.7 13	1550	3.84E-11	4.0 13	1755	2.81E-11	4.0 13	1960	2.08E-11	4.9 13
1350	5.83E-11	4.0 13	1555	4.05E-11	4.7 13	1760	2.82E-11	3.2 13	1965	2.06E-11	5.3 13
1355	5.86E-11	2.5 13	1560	4.00E-11	3.8 13	1765	2.82E-11	4.7 13	1970	2.06E-11	6.1 13

LAMBDA	FLUX	SIGMA NO.	LAMBDA	FLUX	SIGMA NO.	LAMBDA	FLUX	SIGMA NO.	LAMBDA	FLUX	SIGMA NO.
LWR											
1900	2.25E-11	8.8 13	2160	1.51E-11	2.5 7	2420	1.06E-11	4.7 13	2680	8.38E-12	6.2 8
1905	2.13E-11	10.2 13	2165	1.41E-11	4.2 7	2425	1.06E-11	5.2 13	2685	8.24E-12	1.8 7
1910	2.13E-11	7.9 13	2170	1.47E-11	3.2 7	2430	1.12E-11	4.6 13	2690	8.20E-12	3.2 7
1915	2.00E-11	10.3 13	2175	1.54E-11	2.6 7	2435	1.14E-11	5.1 13	2695	7.91E-12	3.7 7
1920	2.13E-11	6.8 13	2180	1.47E-11	5.6 7	2440	1.08E-11	4.9 13	2700	7.74E-12	3.0 7
1925	2.22E-11	7.2 13	2185	1.41E-11	7.4 7	2445	1.09E-11	4.7 13	2705	7.95E-12	4.3 8
1930	2.33E-11	8.0 13	2190	1.46E-11	8.1 11	2450	1.11E-11	3.9 13	2710	7.49E-12	3.5 11
1935	2.15E-11	9.0 13	2195	1.51E-11	11.0 13	2455	1.10E-11	6.5 13	2715	7.36E-12	4.2 13
1940	2.05E-11	8.5 13	2200	1.53E-11	7.3 13	2460	1.10E-11	5.6 13	2720	7.29E-12	3.5 13
1945	2.02E-11	7.2 13	2205	1.42E-11	5.9 13	2465	1.09E-11	4.2 13	2725	6.83E-12	4.0 13
1950	2.05E-11	6.2 10	2210	1.37E-11	4.6 13	2470	1.03E-11	4.8 13	2730	6.22E-12	5.9 13
1955	2.14E-11	5.4 8	2215	1.26E-11	5.1 13	2475	9.88E-12	6.7 13	2735	6.08E-12	4.0 13
1960	2.11E-11	4.7 8	2220	1.29E-11	7.5 13	2480	1.03E-11	4.0 13	2740	6.61E-12	3.8 13
1965	2.00E-11	3.5 8	2225	1.37E-11	10.4 13	2485	1.02E-11	6.5 13	2745	7.00E-12	6.1 13
1970	1.96E-11	4.5 8	2230	1.40E-11	6.0 13	2490	9.90E-12	4.9 13	2750	7.25E-12	3.8 13
1975	2.03E-11	7.5 8	2235	1.37E-11	5.2 13	2495	9.50E-12	5.0 13	2755	7.13E-12	5.2 13
1980	1.96E-11	8.6 11	2240	1.32E-11	8.3 13	2500	1.03E-11	3.9 13	2760	6.92E-12	5.6 13
1985	1.96E-11	7.7 13	2245	1.26E-11	5.1 13	2505	9.42E-12	5.4 13	2765	7.23E-12	7.8 13
1990	2.00E-11	6.5 13	2250	1.20E-11	10.9 13	2510	8.14E-12	3.0 13	2770	7.33E-12	6.9 13
1995	1.97E-11	6.1 13	2255	1.21E-11	8.2 13	2515	8.25E-12	4.6 13	2775	7.13E-12	5.8 13
2000	1.88E-11	5.7 13	2260	1.36E-11	6.6 13	2520	8.89E-12	4.4 13	2780	7.09E-12	6.2 12
2005	1.90E-11	6.6 13	2265	1.38E-11	5.6 13	2525	9.20E-12	4.4 13	2785	6.92E-12	5.2 10
2010	1.91E-11	6.1 13	2270	1.37E-11	5.1 13	2530	9.84E-12	2.7 13	2790	7.09E-12	8.4 10
2015	1.90E-11	6.6 13	2275	1.40E-11	7.2 13	2535	9.56E-12	4.4 13	2795	7.01E-12	6.9 10
2020	1.88E-11	3.9 13	2280	1.42E-11	8.6 13	2540	9.49E-12	2.2 13	2800	6.57E-12	2.8 10
2025	1.88E-11	5.2 13	2285	1.33E-11	5.5 13	2545	9.39E-12	4.2 13	2805	6.64E-12	5.1 12
2030	1.84E-11	4.7 13	2290	1.34E-11	6.1 13	2550	9.66E-12	3.6 13	2810	6.56E-12	5.5 13
2035	1.84E-11	5.3 13	2295	1.30E-11	7.4 13	2555	9.50E-12	2.6 13	2815	6.86E-12	4.9 13
2040	1.85E-11	4.6 13	2300	1.25E-11	7.7 13	2560	9.01E-12	4.8 13	2820	6.73E-12	6.2 13
2045	1.85E-11	4.7 13	2305	1.16E-11	10.4 13	2565	9.54E-12	3.6 10	2825	6.38E-12	5.8 13
2050	1.82E-11	6.3 13	2310	1.20E-11	10.4 13	2570	9.58E-12	5.0 6	2830	6.35E-12	5.1 13
2055	1.74E-11	5.1 10	2315	1.21E-11	6.8 13	2575	9.20E-12	5.3 6	2835	6.44E-12	3.7 13
2060	1.74E-11	5.9 13	2320	1.23E-11	5.5 13	2580	9.27E-12	5.4 6	2840	6.43E-12	5.2 13
2065	1.75E-11	5.4 10	2325	1.30E-11	7.1 13	2585	8.90E-12	3.6 6	2845	6.40E-12	3.8 13
2070	1.72E-11	4.6 10	2330	1.30E-11	7.1 13</td						

TABLE 2C
HD 93521

LAMBDA	FLUX	SIGMA NO.									
SWP											
1155	3.34E-10	9.4 28	1360	2.74E-10	4.2 28	1565	1.32E-10	9.3 28	1770	1.41E-10	4.3 28
1160	3.49E-10	10.1 28	1365	2.76E-10	4.1 28	1570	1.38E-10	6.6 28	1775	1.43E-10	4.4 28
1165	3.42E-10	6.9 28	1370	2.76E-10	4.1 28	1575	1.52E-10	3.3 23	1780	1.41E-10	5.2 13
1170	2.79E-10	7.4 28	1375	2.68E-10	4.6 28	1580	1.52E-10	2.7 15	1785	1.38E-10	3.7 13
1175	2.17E-10	6.3 28	1380	2.64E-10	3.2 28	1585	1.59E-10	3.7 15	1790	1.35E-10	3.4 13
1180	2.70E-10	7.1 19	1385	2.52E-10	3.5 28	1590	1.59E-10	4.4 15	1795	1.32E-10	4.4 13
1185	2.77E-10	5.9 13	1390	1.86E-10	9.5 28	1595	1.50E-10	3.1 15	1800	1.35E-10	4.4 26
1190	2.79E-10	7.0 13	1395	1.77E-10	7.0 28	1600	1.42E-10	3.8 28	1805	1.33E-10	4.9 28
1195	2.59E-10	4.8 13	1400	1.71E-10	8.1 28	1605	1.23E-10	4.4 28	1810	1.28E-10	4.7 28
1200	2.31E-10	5.6 13	1405	1.97E-10	7.9 28	1610	1.09E-10	5.8 28	1815	1.34E-10	4.1 28
1205	2.06E-10	5.4 28	1410	2.29E-10	3.7 28	1615	1.07E-10	7.6 28	1820	1.37E-10	3.9 28
1210	1.86E-10	9.9 28	1415	2.28E-10	4.8 28	1620	1.11E-10	5.3 28	1825	1.31E-10	4.2 28
1215	1.14E-10	8.5 28	1420	2.21E-10	4.0 28	1625	1.12E-10	4.0 28	1830	1.30E-10	3.9 28
1220	2.17E-10	17.0 28	1425	2.13E-10	5.9 28	1630	1.06E-10	4.6 28	1835	1.37E-10	3.5 28
1225	3.14E-10	5.4 28	1430	2.06E-10	4.2 28	1635	1.17E-10	5.3 28	1840	1.29E-10	3.4 28
1230	3.27E-10	5.1 28	1435	2.23E-10	5.0 28	1640	1.24E-10	3.4 28	1845	1.25E-10	3.1 28
1235	2.92E-10	4.6 28	1440	2.25E-10	6.2 28	1645	1.34E-10	4.2 28	1850	1.20E-10	4.3 28
1240	3.07E-10	9.6 28	1445	2.20E-10	4.6 26	1650	1.35E-10	2.6 19	1855	1.13E-10	4.8 28
1245	3.72E-10	2.8 28	1450	2.13E-10	4.5 15	1655	1.24E-10	3.6 13	1860	1.16E-10	3.8 28
1250	3.16E-10	4.1 28	1455	2.03E-10	3.7 15	1660	1.15E-10	3.3 13	1865	1.21E-10	3.3 28
1255	3.02E-10	3.3 28	1460	2.05E-10	3.9 15	1665	1.24E-10	4.7 20	1870	1.23E-10	3.9 28
1260	3.13E-10	3.8 28	1465	2.11E-10	4.6 26	1670	1.24E-10	5.0 28	1875	1.18E-10	4.0 28
1265	3.43E-10	3.0 28	1470	2.16E-10	5.9 28	1675	1.25E-10	5.1 28	1880	1.22E-10	4.0 28
1270	3.48E-10	2.5 28	1475	2.21E-10	5.0 28	1680	1.46E-10	4.1 28	1885	1.13E-10	4.8 28
1275	3.46E-10	2.2 27	1480	2.25E-10	4.7 28	1685	1.46E-10	5.2 28	1890	1.10E-10	5.7 28
1280	3.41E-10	3.6 27	1485	2.23E-10	5.0 28	1690	1.37E-10	5.2 28	1895	1.13E-10	4.7 28
1285	3.30E-10	3.3 28	1490	2.29E-10	4.6 28	1695	1.31E-10	3.9 28	1900	1.16E-10	4.4 28
1290	3.19E-10	3.1 28	1495	2.17E-10	4.5 28	1700	1.28E-10	3.8 28	1905	1.16E-10	4.7 28
1295	2.83E-10	3.7 28	1500	1.97E-10	4.8 28	1705	1.30E-10	3.7 28	1910	1.14E-10	4.1 28
1300	2.55E-10	4.3 28	1505	2.00E-10	4.2 28	1710	1.25E-10	3.3 28	1915	1.10E-10	5.0 20
1305	2.85E-10	5.0 28	1510	2.17E-10	4.7 28	1715	1.19E-10	2.9 28	1920	1.07E-10	5.5 13
1310	3.23E-10	2.8 28	1515	2.12E-10	5.7 28	1720	1.10E-10	4.2 28	1925	1.05E-10	5.2 13
1315	3.16E-10	3.1 27	1520	2.11E-10	6.6 28	1725	1.15E-10	4.2 28	1930	1.08E-10	5.1 13
1320	3.09E-10	3.9 26	1525	1.81E-10	6.4 28	1730	1.31E-10	4.2 28	1935	1.15E-10	4.1 15
1325	3.06E-10	2.9 26	1530	1.55E-10	5.9 28	1735	1.40E-10	3.0 28	1940	1.13E-10	4.0 28
1330	2.98E-10	2.8 28	1535	1.43E-10	4.4 28	1740	1.38E-10	3.5 28	1945	1.14E-10	3.4 28
1335	2.63E-10	3.8 28	1540	1.43E-10	5.3 28	1745	1.38E-10	3.8 28	1950	1.13E-10	3.6 28
1340	2.79E-10	4.2 28	1545	8.79E-11	12.7 28	1750	1.30E-10	4.4 28	1955	1.08E-10	3.9 28
1345	2.79E-10	4.4 28	1550	9.50E-11	18.2 28	1755	1.36E-10	4.8 28	1960	1.07E-10	4.2 28
1350	2.86E-10	3.0 28	1555	1.83E-10	6.0 28	1760	1.45E-10	3.9 28	1965	1.10E-10	5.2 28
1355	2.87E-10	2.7 28	1560	1.52E-10	7.4 28	1765	1.41E-10	4.3 28	1970	1.16E-10	6.4 28

LAMBDA	FLUX	SIGMA NO.									
LWR											
1900	1.11E-10	17.5 26	2160	9.68E-11	5.1 13	2420	7.25E-11	5.9 26	2680	5.59E-11	5.0 19
1905	1.13E-10	13.2 26	2165	9.10E-11	3.3 13	2425	7.12E-11	5.4 26	2685	5.68E-11	5.0 15
1910	1.14E-10	15.1 26	2170	9.51E-11	5.6 13	2430	7.35E-11	7.3 26	2690	5.56E-11	5.9 15
1915	1.02E-10	16.9 26	2175	9.53E-11	8.0 13	2435	7.33E-11	7.1 26	2695	5.36E-11	3.2 15
1920	1.02E-10	13.9 26	2180	9.18E-11	6.1 13	2440	7.26E-11	5.3 26	2700	5.20E-11	4.6 15
1925	1.06E-10	7.4 26	2185	9.74E-11	5.5 13	2445	7.28E-11	4.5 26	2705	5.35E-11	5.4 20
1930	1.15E-10	10.4 26	2190	9.92E-11	11.0 19	2450	7.39E-11	4.3 26	2710	5.40E-11	4.8 26
1935	1.12E-10	9.2 26	2195	9.45E-11	15.8 26	2455	7.41E-11	6.9 26	2715	5.36E-11	5.5 26
1940	1.08E-10	7.4 26	2200	9.24E-11	8.1 26	2460	7.37E-11	6.9 26	2720	5.33E-11	5.3 26
1945	1.10E-10	7.5 26	2205	8.96E-11	7.8 26	2465	7.27E-11	6.6 26	2725	5.19E-11	3.4 26
1950	1.14E-10	7.7 24	2210	9.29E-11	6.8 26	2470	7.05E-11	6.3 26	2730	5.03E-11	4.5 26
1955	1.11E-10	7.5 19	2215	8.94E-11	5.4 26	2475	6.92E-11	4.5 26	2735	5.00E-11	4.0 26
1960	1.02E-10	6.6 19	2220	8.79E-11	6.3 26	2480	6.86E-11	5.6 26	2740	5.06E-11	4.5 26
1965	1.00E-10	8.0 19	2225	8.93E-11	6.4 26	2485	7.02E-11	5.9 26	2745	5.09E-11	3.7 26
1970	1.09E-10	5.6 19	2230	8.77E-11	6.6 26	2490	6.72E-11	7.2 26	2750	5.13E-11	3.7 26
1975	1.16E-10	10.6 20	2235	8.53E-11	5.7 26	2495	6.64E-11	5.4 26	2755	5.10E-11	4.2 26
1980	1.12E-10	9.8 26	2240	8.13E-11	7.6 26	2500	7.06E-11	6.4 26	2760	4.86E-11	4.5 26
1985	1.09E-10	9.2 26	2245	8.26E-11	6.4 26	2505	6.79E-11	5.5 26	2765	4.89E-11	5.2 26
1990	1.05E-10	8.0 26	2250	8.27E-11	9.4 26	2510	6.55E-11	3.3 26	2770	5.01E-11	6.6 26
1995	1.03E-10	6.8 26	2255	8.63E-11	8.2 26	2515	6.37E-11	5.1 26	2775	5.00E-11	3.2 26
2000	1.06E-10	5.7 26	2260	8.96E-11	6.9 26	2520	6.26E-11	5.3 26	2780	5.04E-11	4.9 23
2005	1.11E-10	5.4 26	2265	8.76E-11	7.4 26	2525	6.45E-11	5.4 26	2785	4.84E-11	5.4 20
2010	1.10E-10	5.0 26	2270	8.27E-11	6.4 26	2530	6.70E-11	4.6 26	2790	4.78E-11	8.9 20
2015	1.11E-10	8.0 26	2275	8.65E-11	7.5 26	2535	6.63E-11	5.8 26	2795	4.46E-11	7.3 20
2020	1.13E-10	6.7 26	2280	8.74E-11	6.8 26	2540	6.37E-11	5.0 26	2800	4.21E-11	5.7 20
2025	1.15E-10	7.1 26	2285	8.16E-11	4.9 26	2545	6.33E-11	4.3 26	2805	4.37E-11	5.0 21
2030	1.11E-10	6.0 26	2290	7.93E-11	5.0 26	2550	6.61E-11	4.7 26	2810	4.47E-11	5.2 26
2035	1.08E-10	7.8 26	2295	7.21E-11	7.7 26	2555	6.31E-11	3.3 26	2815	4.88E-11	5.0 26
2040	1.08E-10	7.1 26	2300	7.32E-11	7.4 26	2560	6.07E-11	4.2 26	2820	4.89E-11	4.4 26
2045	1.10E-10	8.2 26	2305	7.90E-11	7.7 26	2565	6.42E-11	4.0 18	2825	4.65E-11	6.1 26
2050	1.08E-10	5.7 21	2310	8.21E-11	5.8 26	2570	6.30E-11	3.8 13	2830	4.50E-11	5.6 26
2055	1.04E-10	4.4 19	2315	8.01E-11	7.7 26	2575	6.33E-11	6.3 13	2835	4.59E-11	4.0 26
2060	1.03E-10	6.0 19	2320	8.19E-11	7.3 26	2580	6.21E-11	4.7 13	2840	4.66E-11	6.4 26
2065	1.02E-10	6.1 19	2325	8.53E-11	4.7 26	2585	5.87E-11	3.0 13	2845	4.60E-11	5.4 26
2070	9.92E-										

TABLE 2D
BD +33°2642

LAMBDA	FLUX	SIGMA NO.	LAMBDA	FLUX	SIGMA NO.	LAMBDA	FLUX	SIGMA NO.	LAMBDA	FLUX	SIGMA NO.
SWP											
1155	4.03E-12	15.1	12	1360	3.66E-12	4.3	12	1565	2.67E-12	4.3	12
1160	4.31E-12	15.3	12	1365	3.66E-12	4.7	12	1570	2.69E-12	3.8	12
1165	4.12E-12	11.3	12	1370	3.58E-12	3.4	12	1575	2.74E-12	5.1	9
1170	3.78E-12	7.9	12	1375	3.47E-12	3.6	12	1580	2.59E-12	4.4	8
1175	3.10E-12	10.3	12	1380	3.50E-12	4.5	12	1585	2.69E-12	3.0	8
1180	3.85E-12	6.8	4	1385	3.54E-12	3.9	12	1590	2.68E-12	2.5	8
1185	3.93E-12	9.5	4	1390	3.15E-12	4.0	12	1595	2.91E-12	3.9	8
1190	3.77E-12	3.8	4	1395	2.92E-12	5.4	12	1600	2.49E-12	5.3	12
1195	3.20E-12	4.0	4	1400	3.06E-12	4.1	12	1605	2.40E-12	5.2	12
1200	2.80E-12	4.9	4	1405	3.17E-12	3.7	12	1610	2.32E-12	4.8	12
1205	2.46E-12	7.8	12	1410	3.36E-12	4.0	12	1615	2.46E-12	6.4	12
1210	2.18E-12	18.4	12	1415	3.29E-12	4.8	12	1620	2.39E-12	4.6	12
1215	1.89E-12	39.1	12	1420	3.29E-12	2.7	12	1625	2.37E-12	3.9	12
1220	2.73E-12	27.8	12	1425	3.38E-12	3.5	12	1630	2.43E-12	2.1	12
1225	3.66E-12	10.1	12	1430	3.39E-12	3.2	12	1635	2.40E-12	4.9	12
1230	3.94E-12	7.6	12	1435	3.39E-12	2.8	12	1640	2.35E-12	2.7	12
1235	4.18E-12	7.6	12	1440	3.42E-12	3.6	12	1645	2.38E-12	4.2	12
1240	4.21E-12	5.1	12	1445	3.37E-12	3.9	11	1650	2.31E-12	2.9	8
1245	4.08E-12	5.4	12	1450	3.39E-12	2.6	8	1655	2.40E-12	2.8	4
1250	3.90E-12	4.5	12	1455	3.34E-12	3.4	8	1660	2.38E-12	4.9	4
1255	3.80E-12	4.8	12	1460	3.31E-12	2.0	8	1665	2.27E-12	4.6	5
1260	3.63E-12	5.4	12	1465	3.29E-12	5.3	12	1670	2.20E-12	2.8	12
1265	3.98E-12	4.2	12	1470	3.32E-12	8.0	12	1675	2.22E-12	2.9	12
1270	4.25E-12	2.7	12	1475	3.17E-12	2.8	12	1680	2.36E-12	4.7	12
1275	4.13E-12	3.8	12	1480	3.34E-12	5.1	12	1685	2.33E-12	4.7	12
1280	4.21E-12	2.5	12	1485	3.31E-12	6.5	12	1690	2.31E-12	5.9	12
1285	4.15E-12	2.9	12	1490	3.31E-12	4.6	12	1695	2.37E-12	2.6	12
1290	3.91E-12	5.5	12	1495	3.24E-12	3.4	12	1700	2.34E-12	3.6	12
1295	3.63E-12	5.6	12	1500	3.03E-12	2.3	12	1705	2.29E-12	3.2	12
1300	3.22E-12	5.4	12	1505	2.93E-12	4.1	12	1710	2.22E-12	2.8	12
1305	3.52E-12	8.9	12	1510	2.94E-12	3.3	12	1715	2.10E-12	3.5	12
1310	4.07E-12	4.7	12	1515	2.95E-12	4.0	12	1720	2.08E-12	2.9	12
1315	4.14E-12	7.2	12	1520	2.99E-12	5.8	12	1725	2.14E-12	5.6	12
1320	3.90E-12	3.0	11	1525	2.86E-12	3.3	12	1730	2.26E-12	4.2	12
1325	3.72E-12	3.5	11	1530	2.75E-12	4.4	12	1735	2.28E-12	2.9	12
1330	3.63E-12	5.4	12	1535	2.70E-12	5.7	12	1740	2.22E-12	2.7	12
1335	3.29E-12	5.6	12	1540	2.71E-12	5.9	12	1745	2.24E-12	2.6	12
1340	3.60E-12	5.1	12	1545	2.57E-12	4.0	12	1750	2.20E-12	3.5	12
1345	3.62E-12	6.4	12	1550	2.45E-12	4.3	12	1755	2.25E-12	5.1	12
1350	3.75E-12	3.9	12	1555	2.78E-12	6.8	12	1760	2.26E-12	3.2	12
1355	3.75E-12	2.3	12	1560	2.72E-12	3.9	12	1765	2.28E-12	3.8	12

LAMBDA	FLUX	SIGMA NO.	LAMBDA	FLUX	SIGMA NO.	LAMBDA	FLUX	SIGMA NO.	LAMBDA	FLUX	SIGMA NO.
LWR											
1900	1.51E-12	19.9	11	2160	1.51E-12	8.1	7	2420	1.20E-12	4.0	11
1905	1.53E-12	16.1	11	2165	1.40E-12	5.4	7	2425	1.19E-12	5.1	11
1910	1.55E-12	18.5	11	2170	1.42E-12	6.2	7	2430	1.19E-12	5.1	11
1915	1.40E-12	24.7	11	2175	1.42E-12	6.9	7	2435	1.19E-12	4.8	11
1920	1.40E-12	28.3	11	2180	1.45E-12	4.3	7	2440	1.15E-12	5.9	11
1925	1.57E-12	18.9	11	2185	1.55E-12	6.9	7	2445	1.23E-12	5.9	11
1930	1.72E-12	20.0	11	2190	1.64E-12	12.6	9	2450	1.26E-12	4.1	11
1935	1.73E-12	16.1	11	2195	1.57E-12	18.0	11	2455	1.26E-12	5.3	11
1940	1.64E-12	10.0	11	2200	1.49E-12	8.6	11	2460	1.23E-12	7.3	11
1945	1.71E-12	8.7	11	2205	1.40E-12	7.1	11	2465	1.21E-12	7.7	11
1950	1.83E-12	7.2	8	2210	1.44E-12	8.0	11	2470	1.15E-12	5.6	11
1955	1.74E-12	10.2	7	2215	1.37E-12	6.3	11	2475	1.11E-12	7.5	11
1960	1.69E-12	11.7	7	2220	1.27E-12	7.3	11	2480	1.15E-12	5.7	11
1965	1.62E-12	10.8	7	2225	1.31E-12	6.5	11	2485	1.13E-12	5.8	11
1970	1.72E-12	9.6	7	2230	1.33E-12	5.9	11	2490	1.11E-12	4.9	11
1975	1.91E-12	9.5	7	2235	1.26E-12	6.5	11	2495	1.06E-12	4.3	11
1980	1.77E-12	9.9	10	2240	1.26E-12	10.0	11	2500	1.20E-12	5.5	11
1985	1.71E-12	11.4	11	2245	1.28E-12	4.7	11	2505	1.18E-12	4.6	11
1990	1.68E-12	7.9	11	2250	1.33E-12	9.9	11	2510	1.10E-12	3.8	11
1995	1.56E-12	10.5	11	2255	1.36E-12	7.6	11	2515	1.06E-12	5.6	11
2000	1.53E-12	8.4	11	2260	1.39E-12	3.6	11	2520	1.06E-12	5.2	11
2005	1.64E-12	7.5	11	2265	1.35E-12	7.6	11	2525	1.06E-12	4.7	11
2010	1.65E-12	8.2	11	2270	1.36E-12	7.4	11	2530	1.09E-12	5.7	11
2015	1.61E-12	8.7	11	2275	1.44E-12	6.8	11	2535	1.09E-12	4.5	11
2020	1.67E-12	4.1	11	2280	1.45E-12	9.2	11	2540	1.08E-12	4.8	11
2025	1.67E-12	6.1	11	2285	1.34E-12	11.7	11	2545	1.09E-12	6.8	11
2030	1.66E-12	7.4	11	2290	1.33E-12	3.9	11	2550	1.11E-12	6.8	11
2035	1.58E-12	12.0	11	2295	1.35E-12	5.6	11	2555	1.05E-12	5.5	11
2040	1.57E-12	9.8	11	2300	1.33E-12	9.4	11	2560	1.04E-12	7.4	11
2045	1.62E-12	7.8	11	2305	1.38E-12	6.4	11	2565	1.09E-12	4.8	10
2050	1.63E-12	5.0	11	2310	1.41E-12	20.4	11	2570	1.08E-12	5.3	4
2055	1.66E-12	7.3	6	2315	1.36E-12	17.1	11	2575	1.04E-12	2.9	4
2060	1.61E-12	7.2	6	2320	1.31E-12	7.3	11	2580	1.02E-12	3.8	4
2065	1.53E-12	6.1	6	2325	1.37E-12	6.9	11	2585	1.01E-12	2.9	4
2070	1.52E-12	7.0	6	2330	1.35E-12	7.9	11	2590	9.92E-13	4.6	4
2075	1.58E-12	4.8	6	2335	1.32E-12	6.2	11	2595	9.57E-13	3.8	4
2080	1.69E-12	6.4	11	2340	1.24E-12	5.8	11	2600	9.74E-13	2.5	4
2085	1.54E-12	6.1	11	2345	1.20E-12	6.9	11	2605	1.02E-12	3.2	9
2090	1.56E-12	6.5	11	2350	1.28E-12	6.5	11	2610	1.06E-12	2.8	11
2095	1.54E-12	6.9	11	2355	1.30E-12	3.0	11	2615	1.08E-12	4.2	11
2100	1.46E-12	6.0	11	2360	1.37E-12	4.4	11	2620	1.06E-12	5.3	11
2105	1.47E-12	9.6	11	2365	1.25E-12	4.4	11	2625	1.02E-12	4.5	11
2110	1.60E-12	5.5	11	2370	1.25E-12	6.7	11	2630	1.03E-12	2.3	11
2115	1.52E-12	4.3	11	2375	1.19E-12	5.5	11	2635	1.03E-12	4.7	11
2120	1.44E-12	6.0	11	2380	1.13E-12	5.9	11	2640	9.99E-13	3.9	11
2125	1.55E-12	6.8	11	2385	1.12E-12	5.9	11	2645	9.75E-13	5.7	11
2130	1.51E-12	12.8	11	2390	1.18E-12	6.5	11	2650	1.01E-12	4.8	11
2135	1.50E-12	7.9	11	2395	1.19E-12	9.1	11	2655	1.06E-12	5.6	11
2140											

TABLE 2E
BD +28°4211

LAMBDA	FLUX	SIGMA NO.									
SWP											
1155	7.08E-11	10.9 24	1360	3.80E-11	5.1 24	1565	2.32E-11	4.9 24	1770	1.46E-11	4.8 24
1160	6.98E-11	13.3 24	1365	3.74E-11	5.3 24	1570	2.28E-11	4.7 24	1775	1.44E-11	3.7 23
1165	6.74E-11	11.6 24	1370	3.52E-11	5.0 24	1575	2.31E-11	5.9 16	1780	1.42E-11	4.2 12
1170	6.71E-11	8.4 24	1375	3.51E-11	4.8 24	1580	2.22E-11	6.1 12	1785	1.42E-11	4.0 12
1175	6.79E-11	7.4 24	1380	3.62E-11	5.0 24	1585	2.18E-11	6.1 12	1790	1.41E-11	2.3 12
1180	6.81E-11	7.1 19	1385	3.61E-11	4.5 24	1590	2.10E-11	5.3 12	1795	1.40E-11	3.6 13
1185	6.65E-11	8.5 13	1390	3.48E-11	4.8 24	1595	2.05E-11	4.7 13	1800	1.38E-11	3.6 19
1190	6.43E-11	7.6 12	1395	3.42E-11	4.4 24	1600	2.05E-11	5.3 24	1805	1.36E-11	5.0 24
1195	6.08E-11	6.4 12	1400	3.45E-11	5.2 24	1605	1.97E-11	6.2 24	1810	1.34E-11	5.0 24
1200	6.02E-11	6.2 12	1405	3.32E-11	4.8 24	1610	1.93E-11	5.4 24	1815	1.33E-11	4.9 24
1205	5.70E-11	5.7 23	1410	3.32E-11	4.9 24	1615	1.87E-11	4.7 24	1820	1.34E-11	3.9 24
1210	4.24E-11	17.4 24	1415	3.21E-11	4.3 24	1620	1.79E-11	5.1 24	1825	1.29E-11	4.3 24
1215	2.84E-11	14.4 24	1420	3.21E-11	4.3 24	1625	1.80E-11	4.4 24	1830	1.29E-11	4.3 24
1220	4.20E-11	21.0 24	1425	3.26E-11	5.4 24	1630	1.80E-11	5.1 24	1835	1.27E-11	4.5 24
1225	5.35E-11	8.2 24	1430	3.24E-11	3.4 24	1635	1.68E-11	5.3 24	1840	1.25E-11	3.6 24
1230	5.57E-11	6.0 24	1435	3.22E-11	4.7 24	1640	1.55E-11	6.0 24	1845	1.25E-11	4.5 24
1235	5.30E-11	4.6 24	1440	3.10E-11	6.2 24	1645	1.63E-11	7.2 23	1850	1.22E-11	4.8 24
1240	4.89E-11	4.8 24	1445	3.04E-11	5.4 21	1650	1.68E-11	5.1 15	1855	1.19E-11	4.7 24
1245	5.24E-11	6.4 24	1450	3.02E-11	4.6 12	1655	1.72E-11	3.6 12	1860	1.20E-11	5.2 24
1250	5.37E-11	3.9 24	1455	3.02E-11	3.5 12	1660	1.70E-11	4.3 12	1865	1.20E-11	4.4 24
1255	5.26E-11	4.3 24	1460	2.90E-11	4.2 12	1665	1.67E-11	4.5 19	1870	1.19E-11	5.2 24
1260	5.17E-11	5.7 24	1465	2.94E-11	4.6 22	1670	1.69E-11	4.2 24	1875	1.16E-11	5.6 24
1265	5.23E-11	4.2 24	1470	2.97E-11	5.4 24	1675	1.65E-11	5.3 24	1880	1.15E-11	4.6 24
1270	5.17E-11	3.9 24	1475	2.89E-11	4.5 24	1680	1.63E-11	5.0 24	1885	1.11E-11	5.4 24
1275	5.07E-11	5.6 24	1480	2.96E-11	4.4 24	1685	1.61E-11	5.7 24	1890	1.11E-11	5.6 24
1280	5.08E-11	4.7 24	1485	2.90E-11	4.8 24	1690	1.65E-11	5.2 24	1895	1.10E-11	4.7 24
1285	4.94E-11	3.8 24	1490	2.93E-11	4.9 24	1695	1.64E-11	4.3 24	1900	1.08E-11	5.6 24
1290	4.80E-11	4.6 24	1495	2.91E-11	3.5 24	1700	1.61E-11	4.6 24	1905	1.04E-11	6.2 24
1295	4.74E-11	5.3 24	1500	2.79E-11	4.3 24	1705	1.57E-11	4.3 24	1910	1.04E-11	5.4 23
1300	4.62E-11	3.0 24	1505	2.68E-11	4.5 24	1710	1.57E-11	4.1 24	1915	1.06E-11	6.4 17
1305	4.57E-11	4.1 24	1510	2.68E-11	4.9 24	1715	1.53E-11	4.8 24	1920	1.04E-11	4.5 12
1310	4.55E-11	5.3 24	1515	2.68E-11	6.3 24	1720	1.52E-11	5.3 24	1925	1.01E-11	6.0 13
1315	4.56E-11	5.3 23	1520	2.68E-11	6.0 24	1725	1.54E-11	4.3 24	1930	1.03E-11	5.8 13
1320	4.52E-11	4.5 21	1525	2.65E-11	4.8 24	1730	1.55E-11	3.6 24	1935	1.01E-11	4.2 16
1325	4.38E-11	4.8 21	1530	2.63E-11	6.3 24	1735	1.55E-11	4.7 24	1940	9.88E-12	5.8 24
1330	4.22E-11	4.9 24	1535	2.62E-11	6.5 24	1740	1.51E-11	3.5 24	1945	1.01E-11	5.6 24
1335	3.97E-11	3.8 24	1540	2.54E-11	6.4 24	1745	1.51E-11	3.8 24	1950	1.03E-11	5.3 24
1340	3.96E-11	5.0 24	1545	2.38E-11	6.4 24	1750	1.51E-11	3.4 24	1955	1.03E-11	6.0 24
1345	3.98E-11	5.9 24	1550	2.25E-11	5.1 24	1755	1.49E-11	4.1 24	1960	1.01E-11	5.1 23
1350	3.92E-11	4.2 24	1555	2.45E-11	6.3 24	1760	1.49E-11	4.5 24	1965	9.99E-12	6.2 23
1355	3.88E-11	3.8 24	1560	2.40E-11	4.8 24	1765	1.50E-11	3.8 24	1970	9.86E-12	8.6 23

LAMBDA	FLUX	SIGMA NO.									
LWR											
1900	1.05E-11	14.5 13	2160	6.66E-12	6.5 7	2420	4.66E-12	5.9 13	2680	3.45E-12	6.1 8
1905	1.00E-11	6.4 13	2165	6.53E-12	3.5 7	2425	4.56E-12	4.1 13	2685	3.36E-12	4.5 8
1910	1.02E-11	7.3 13	2170	6.54E-12	4.6 7	2430	4.63E-12	5.5 13	2690	3.45E-12	3.2 8
1915	9.56E-12	9.0 13	2175	6.43E-12	4.3 7	2435	4.61E-12	3.1 13	2695	3.30E-12	5.8 8
1920	9.66E-12	7.8 13	2180	6.17E-12	4.8 7	2440	4.46E-12	4.8 13	2700	3.25E-12	4.5 8
1925	9.85E-12	6.7 13	2185	6.30E-12	6.3 7	2445	4.56E-12	4.1 13	2705	3.33E-12	3.9 8
1930	1.02E-11	7.9 13	2190	6.72E-12	6.7 9	2450	4.67E-12	5.6 13	2710	3.14E-12	4.0 12
1935	9.54E-12	7.0 13	2195	6.25E-12	12.0 13	2455	4.60E-12	6.7 13	2715	3.13E-12	4.5 13
1940	9.33E-12	7.1 13	2200	6.22E-12	6.8 13	2460	4.57E-12	5.9 13	2720	3.10E-12	4.6 13
1945	9.63E-12	8.4 13	2205	6.05E-12	8.3 13	2465	4.43E-12	5.9 13	2725	3.04E-12	3.3 13
1950	9.45E-12	6.5 11	2210	6.00E-12	7.4 13	2470	4.24E-12	6.2 13	2730	2.91E-12	6.7 13
1955	9.42E-12	10.0 8	2215	6.03E-12	9.0 13	2475	4.15E-12	6.5 13	2735	2.76E-12	5.0 13
1960	9.15E-12	7.8 8	2220	6.11E-12	8.2 13	2480	4.25E-12	3.9 13	2740	2.85E-12	6.0 13
1965	8.90E-12	2.7 8	2225	5.90E-12	4.8 13	2485	4.23E-12	5.7 13	2745	2.96E-12	4.5 13
1970	9.17E-12	7.6 8	2230	5.78E-12	7.2 13	2490	4.06E-12	6.5 13	2750	3.00E-12	3.6 13
1975	9.35E-12	6.6 8	2235	5.69E-12	5.1 13	2495	3.93E-12	6.1 13	2755	2.94E-12	4.9 13
1980	8.86E-12	8.3 13	2240	5.63E-12	7.1 13	2500	4.26E-12	4.1 13	2760	2.84E-12	6.0 13
1985	8.98E-12	6.8 13	2245	5.45E-12	6.4 13	2505	4.13E-12	4.7 13	2765	2.89E-12	5.6 13
1990	9.12E-12	4.4 13	2250	5.39E-12	9.2 13	2510	3.75E-12	4.6 13	2770	2.93E-12	6.1 13
1995	9.00E-12	4.8 13	2255	5.58E-12	6.9 13	2515	3.71E-12	4.7 13	2775	2.85E-12	4.0 12
2000	8.53E-12	3.2 13	2260	5.83E-12	4.5 13	2520	3.85E-12	5.4 13	2780	2.86E-12	3.2 11
2005	8.55E-12	3.8 13	2265	5.68E-12	6.3 13	2525	3.93E-12	5.1 13	2785	2.79E-12	3.8 11
2010	8.47E-12	4.8 13	2270	5.59E-12	10.5 13	2530	4.02E-12	3.6 13	2790	2.97E-12	7.8 11
2015	8.36E-12	4.6 13	2275	5.79E-12	8.7 13	2535	3.99E-12	5.2 13	2795	2.87E-12	5.9 12
2020	8.54E-12	5.2 13	2280	5.74E-12	7.1 13	2540	3.98E-12	3.2 13	2800	2.75E-12	3.9 12
2025	8.50E-12	8.2 13	2285	5.56E-12	4.7 13	2545	3.98E-12	3.2 13	2805	2.76E-12	5.7 12
2030	8.33E-12	6.2 13	2290	5.53E-12	6.3 13	2550	4.04E-12	3.3 13	2810	2.68E-12	5.6 12
2035	8.24E-12	4.2 13	2295	5.46E-12	5.6 13	2555	3.82E-12	3.1 13	2815	2.83E-12	5.5 13
2040	8.14E-12	6.5 13	2300	5.47E-12	7.6 13	2560	3.77E-12	4.9 13	2820	2.81E-12	6.2 13
2045	8.14E-12	5.1 12	2305	5.34E-12	8.3 13	2565	3.85E-12	4.4 12	2825	2.68E-12	4.9 13
2050	8.27E-12	5.1 12	2310	5.30E-12	6.2 13	2570	3.81E-12	5.2 7	2830	2.63E-12	5.4 13
2055	8.08E-12	7.1 9	2315	5.16E-12	7.2 13	2575	3.94E-12	2.6 2	2835	2.68E-12	4.0 13
2060	8.03E-12	3.4 9	2320	5.21E-12	6.5 13	2580	3.95E-12	2.0 6	2840	2.72E-12	3.9 13
2065	7.86E-12	3.8 10	2325	5.35E-12	6.0 13	2585	3.80E-12	2.0 6	2845	2.71E-12	4.1 13
2070	7.82E-12	2.7 10	2330								

1. The mean epoch of the original *IUE* calibration represented by the fluxes of Table 2 is 1978.8. By assuming that the fluxes of Table 2 reflect the *IUE* sensitivity as of 1978.8, any error is less than 1% due to differential sensitivity change over the 1978 April to 1979 April calibration period.

2. *IUE* exposure times for point source spectra are uncertain by 30 ms due to questions about when the on-board computer turns the high voltage on and off. For the brightest star in the UV, HD 93521, exposure times were as short as 2.75 s in the large aperture. A 30 ms error would make any individual spectrum of HD 93521 uncertain by 1%. However, the fluxes of Table 2 are based on the large-aperture level set by 15 SWP and 13 LWR spectra, which are expected to reduce the 1% by the square root of the number of independent observations. Further evidence to substantiate the validity of HD 93521 as a standard are the values for the mean scatter in the 5 Å bins (see Table 1), which are typical of the values for the other stars.

3. The well-known nonlinearity problems of *IUE* (e.g., Oliversen 1983) may be the dominant source of error in the relative fluxes of the five standards. Since all spectra were exposed to similar levels at one wavelength, since all spectra have a background that is small compared to the net signal, and since all stars are hot and unreddened, linearity errors are minimized. However, residual nonlinearity due to remaining differences in the actual exposure levels and in the slope of the flux distributions as a function of wavelength may be the dominant uncertainty among the relative flux levels of the standards. One measure of the internal accuracy of the standards is to compare the *TD-1* fluxes of Jamar *et al.* (1976) with those in Table 2. This comparison was done in the process of the original calibration, which showed a typical scatter of 3% about the mean. However, BD +28°4211 has both the largest scatter, of up to 7% about the mean calibration curve, and also the most deviant flux distribution. This largest systematic deviation from the mean comparison with *TD-1* as a function of wavelength is indicative of a linearity error for this case of the most extreme shape of the *IUE* response.

III. THE NEW *IUE* ABSOLUTE CALIBRATION

When the small-aperture spectra are corrected to the shape of the large-aperture point source spectra, normalized to the large aperture, and combined to get the proper net spectrum $\sum A$, the resulting stellar fluxes are *not* the same as those that had been derived under the original assumption that the small-aperture response is gray. Assuming that the original fluxes from the point source observations of the five program stars were correctly derived from the *OAO 2* and *TD-1* reference standards, the average ratio of the proper net spectra to the original net spectra define the changes needed to the large-aperture point source calibration. Since the S/L corrections are smoothed on the same 25 Å scale for SWP and 50 Å scale for LWR that was used to derive the original absolute calibration, and since the changes in $\sum A$ are smooth, these corrections to the absolute calibration in Table 3 are also smooth. The smooth S/L and new absolute large-aperture point source calibrations that together maintain the same mean fluxes for the five well-observed *IUE* flux standards are given in Tables 3A and 3B for SWP and LWR respectively. Also included in the table are the smooth T/L corrections for trailed spectra in the large aperture, which were derived using the same techniques as for S/L. The change in the *IUE* absolute calibration as applied to point sources in the large aperture is typically less than 5% below 3100 Å but rises to 10% at 3200 Å.

The fluxes for the five standard stars in Table 2 are based on the new point source absolute calibration and the S/L correction for those small-aperture spectra that are included in the average for each star. See a preliminary version of this paper by Bohlin (1985) for the journal of observations. Although the mean fluxes for the five stars as a group do not change, individual stars do show differences of a few percent, depending on the degree to which small-aperture signal is used to define the net flux. For example, the relative flux at 3200 Å between BD +33°2642 and BD +28°4211 changes by ~5%. Since the five standards are used by the *IUE* project to monitor sensitivity changes, their fluxes in Table 2 for the first-year epoch of *IUE* will be important for setting the precise absolute scale throughout the *IUE* lifetime and, therefore, will define the fluxes of the UV standards for the Hubble Space Telescope.

As a final check on this recalibration of *IUE*, the absolute fluxes were rederived for the stars with *OAO 2* and *TD-1* fluxes that were originally used by Bohlin and Holm (1980) to calibrate *IUE*. See Bohlin and Holm (1984) for the list of stars. These new fluxes from *IUE* spectra that included some trailed observations were compared afresh to the *OAO 2* and *TD-1* reference fluxes. The *IUE* fluxes based on the corrections of Table 3 agree with the original reference spectra to within 3%, which is a small error compared with the 10% uncertainty in the reference standards that are the basis of the *IUE* calibration. Therefore, the new *IUE* calibration in Table 3 accounts only for the inadequacies in the original calibration techniques; no new transfer of *OAO 2* or *TD-1* flux scales to *IUE* has been done.

IV. COMPARISON OF *IUE* FLUXES WITH GROUND-BASED OBSERVATIONS

Since *IUE* lacks sensitivity longward of 3200 Å, and since ground-based spectrophotometry is problematic below 3300 Å, quantitative comparisons require a model that can be fitted to one data set in order to predict fluxes at the wavelengths of the other data set. Figures 1 and 2 show the *IUE* fluxes from Table 2 along with the data of Stone (1977) for BD +28°4211 and BD +33°2642 respectively. The magnitudes per unit frequency interval $m(v)$ from Stone were converted to flux per unit frequency interval $F(v)$ by

$$2.5 \log F(v) = -48.60 - m(v),$$

and then $F(v)$ was converted to $F(\lambda)$ for comparison with *IUE*. The model fit is constrained to pass through the data averaged in a 100 Å bandpass centered at 3050 Å. Beyond 3100 Å, the scatter in the *IUE* flux values begins to increase. A sophisticated model is not needed, since the model is used only to predict the shape of the continuum over the short interval from 3050 Å to the data point of Stone at 3571 Å, where there should be no contamination from light longward of the Balmer limit. One choice of models is the Planck blackbody function that passes through the *IUE* continuum in the 1200–1400 Å region and also through the 3050 Å point. The blackbody functions shown in Figures 1 and 2 that satisfy these constraints are for temperatures of 120,100 and 26,400 K for BD +28°4211 and BD +33°2642 respectively. The mean ratio of the six Stone measurements between 3300 and 3571 Å to the model fitted to the *IUE* data is 0.983, with an rms scatter of 0.009 for BD +28°4211 and 1.011 ± 0.014 for BD +33°2642. The Stone values at 3200 and 3250 Å are discrepant and are not considered, since Stone says that the correction of –0.011 mag he used to place his calibration in the

TABLE 3
ZERO-EPOCH IUE ABSOLUTE CALIBRATION

λ (Å)	Correction ^a	$S^{-1}(\text{LAp})^b$ (10^{-14} ergs cm^{-2} \AA^{-1} FN $^{-1}$)	S/L ^c	T/L ^d	λ (Å)	Correction ^a	$S^{-1}(\text{LAp})^b$ (10^{-14} ergs cm^{-2} \AA^{-1} FN $^{-1}$)	S/L ^c	T/L ^d
A. SWP Camera					B. LWR Camera				
1150.....	1.024	20.2:	0.970	1.069	1850.....	0.953	15.1	1.113	1.048
1175.....	1.018	7.78:	0.977	1.050	1900.....	0.964	5.08	1.063	1.036
1200.....	1.014	4.28:	0.983	1.034	1950.....	0.978	2.85	1.024	1.029
1225.....	1.010	2.89:	0.989	1.019	2000.....	0.988	1.90	0.998	1.024
1250.....	1.007	2.39	0.995	1.005	2050.....	0.994	1.63	0.981	1.020
1275.....	1.005	2.23	0.999	0.997	2100.....	0.998	1.50	0.973	1.017
1300.....	1.004	2.17	1.002	0.991	2150.....	0.999	1.47	0.971	1.013
1325.....	1.003	2.18	1.005	0.990	2200.....	0.999	1.40	0.971	1.010
1350.....	1.002	2.26	1.008	0.991	2250.....	0.999	1.20	0.971	1.007
1375.....	1.000	2.40	1.011	0.996	2300.....	0.998	1.00	0.973	1.003
1400.....	0.999	2.60	1.014	1.002	2350.....	0.993	0.828	0.986	1.000
1425.....	0.998	2.81	1.016	1.007	2400.....	0.986	0.705	1.002	1.000
1450.....	0.998	3.05	1.017	1.012	2450.....	0.980	0.593	1.021	1.000
1475.....	0.997	3.31	1.018	1.018	2500.....	0.975	0.516	1.032	1.000
1500.....	0.997	3.55	1.019	1.027	2550.....	0.973	0.457	1.040	1.000
1525.....	0.997	3.75	1.018	1.036	2600.....	0.970	0.414	1.047	1.003
1550.....	0.997	3.85	1.018	1.048	2650.....	0.968	0.378	1.050	1.006
1575.....	0.998	3.71	1.017	1.051	2700.....	0.968	0.350	1.052	1.010
1600.....	0.998	3.51	1.016	1.052	2750.....	0.969	0.341	1.048	1.013
1625.....	0.999	3.32	1.015	1.053	2800.....	0.971	0.339	1.042	1.017
1650.....	0.999	3.12	1.013	1.052	2850.....	0.974	0.347	1.036	1.020
1675.....	1.000	2.92	1.011	1.049	2900.....	0.976	0.375	1.030	1.024
1700.....	1.001	2.73	1.008	1.042	2950.....	0.979	0.421	1.022	1.028
1725.....	1.003	2.53	1.005	1.035	3000.....	0.982	0.493	1.014	1.032
1750.....	1.004	2.35	1.002	1.030	3050.....	0.987	0.612	1.000	1.038
1775.....	1.005	2.19	0.999	1.028	3100.....	1.010	0.843	0.956	1.038
1800.....	1.007	2.09	0.995	1.027	3150.....	1.057	1.22:	0.825	1.036
1825.....	1.009	2.04	0.990	1.028	3200.....	1.105	1.90:	0.735	1.034
1850.....	1.012	2.02	0.984	1.028	3250.....	1.126	3.38:	0.686	1.032
1875.....	1.014	2.01	0.978	1.027	3300.....	1.130	7.09:	0.642	1.030
1900.....	1.017	2.00	0.972	1.026	3350.....	1.130	15.0:	0.614	1.028
1925.....	1.019	1.98	0.966	1.024					
1950.....	1.022	1.98	0.960	1.022					
1975.....	1.026	1.95	0.954	1.020					

^a Correction to the Bohlin and Holm 1980 calibration $S^{-1}(1980)$, such that the new calibration for point sources centered in the large aperture in the next column is

$$S^{-1}(\text{LAp}) = S^{-1}(1980)/\text{Correction}.$$

^b IUE inverse sensitivities for a point source centered in the large aperture. The stellar flux $F(\lambda)$ in ergs cm^{-2} s^{-1} \AA^{-1} is

$$F(\lambda) = S^{-1}(\lambda) \frac{\text{FN}(\lambda)}{t},$$

where $\text{FN}(\lambda)$ is the linearized IUE response in Flux Numbers and t is the exposure time in seconds.

^c Ratio of small-aperture response to the large-aperture response for point sources. Since the IUE small aperture is not a photometric aperture, the average of S/L over all wavelengths is normalized to unity. The relative small and absolute large aperture inverse sensitivities are related by

$$S^{-1}(\text{SAP}) = S^{-1}(\text{LAp}) / (\text{S/L}).$$

^d Ratio of trailed response to point sources in the large aperture. The absolute calibrations are related by

$$S^{-1}(\text{Trail}) = S^{-1}(\text{LAp}) / (\text{T/L}).$$

The values of T/L are for trailed exposure times computed using lengths for the large apertures of 21''4 for SWP and 20''5 for LWR (Panek 1982).

Balmer continuum on the Hayes and Latham (1975) scale for Vega "has (admittedly rather arbitrarily) been extrapolated to the two extreme ultraviolet points at $\lambda 3200$ and $\lambda 3250$."

Another possibility for modeling the slope of the Balmer continuum from 3050 to 3571 Å is to use model atmosphere computations. In the case of BD +28°4211, the $\log g = 6$, LTE pure helium models of Wesemael (1981) differ in the ratio $F(3571)/F(3050)$ from a blackbody of the same temperature by less than 1% in the 100,000–150,000 K range. In the case of

BD +33°2642, there is a Balmer jump, so that the pure hydrogen, LTE models of Wesemael *et al.* (1980) with hydrogen line blanketing seem more appropriate. For $\log g = 6.0$, a temperature of 20,500 K is deduced from the measured flux ratio between 3050 and 5556 Å. The model for 20,500 K is interpolated from the Wesemael *et al.* (1980) models computed for 20,000 and 30,000 K. The ratio of the Stone fluxes to this model for BD +33°2642 is 1.006 ± 0.012 . Despite the consistency of all the models considered over the narrow

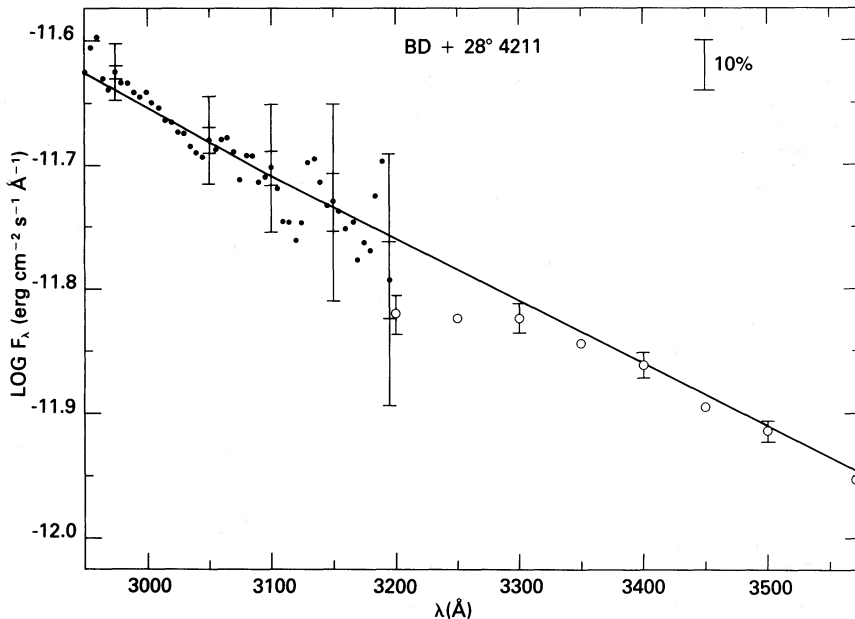


FIG. 1.—*IUE* (filled circles) and ground-based fluxes (open circles) from Stone (1977) for BD + 28°4211. *IUE* data from the first year of operations for seven large- and six small-aperture spectra have been combined in 5 Å bins. The rms scatter of independent observations is shown for the Stone data and as the outer error bar for *IUE*. The inner error bars shown for the sample *IUE* points are estimates of the error in the mean, computed by reducing the rms error by the square root of the 13 independent observations. The solid line is the Planck function for $T = 120,100$ K derived from a fit to the *IUE* data.

3050–3571 Å range, the fits of these models to the *IUE* fluxes are quite bad at other wavelengths. For example, at 1900 Å, the blackbody lies above BD + 28°4211 by 12% and above BD + 33°2642 by 35%. The 20,500 K line-blanketed model atmosphere is even higher than the 26,400 K blackbody in the *IUE* wavelength range when both models are normalized at 3050 Å.

In summary, the *IUE* data for two of the standard stars agree with ground-based data to within 2%. This conclusion is independent of the model used to make the comparisons. Even

if the small interstellar extinction corrections that are allowed by the data are introduced, the conclusion is unaffected.

V. COMPARISON OF *IUE* FLUXES WITH VOYAGER OBSERVATIONS

The *Voyager* spectrophotometry of Holberg *et al.* (1982) overlaps the *IUE* data at the shortest wavelengths, as shown for BD + 28°4211 in Figure 3 and for BD + 75°325 in Figure 4 (Holberg 1985). While all four *Voyager* data points between 1150 and 1200 Å for BD + 28°4211 agree with *IUE* within the

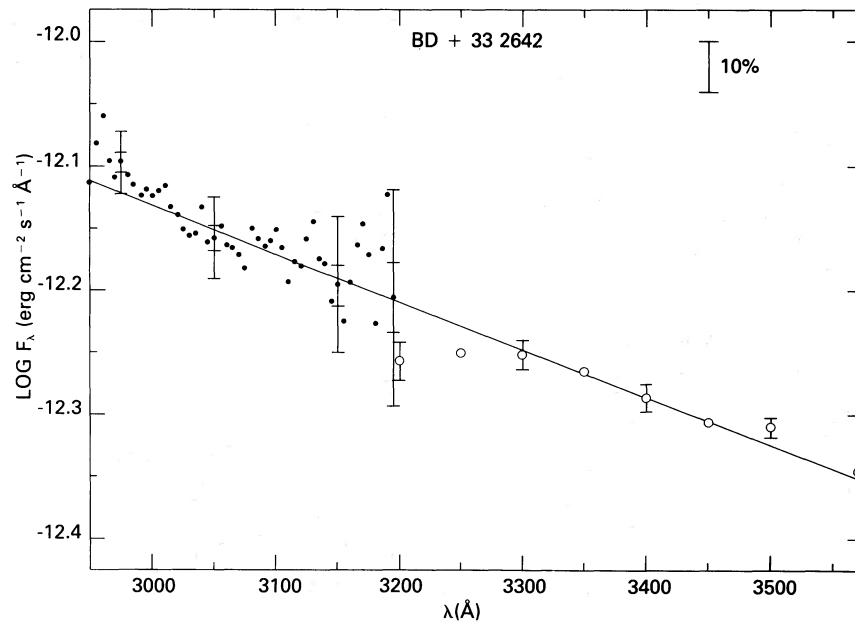


FIG. 2.—Same as Fig. 1, for BD + 33°2642. *IUE* data are combined for seven large- and four small-aperture spectra, while the blackbody fit is for $T = 26,400$ K.

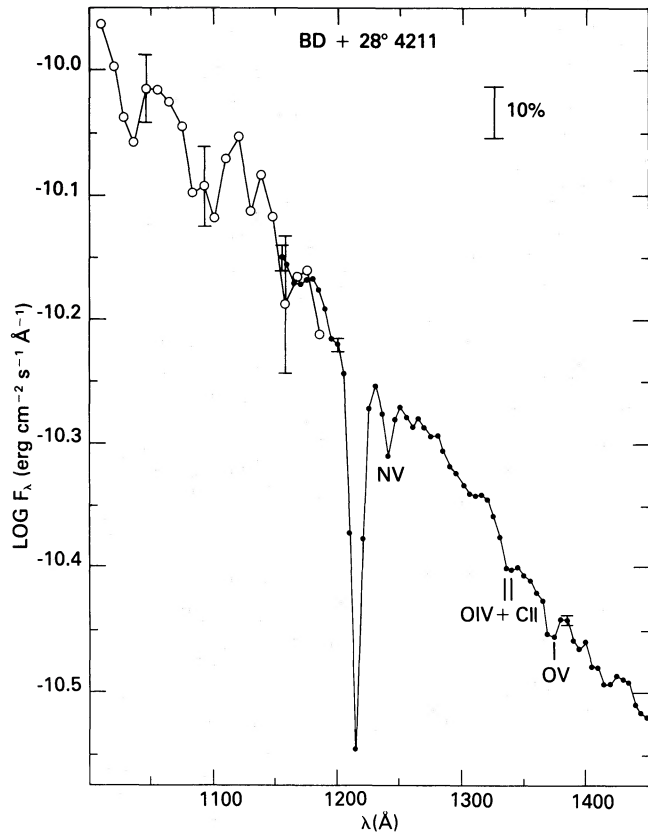


FIG. 3

FIG. 3.—*IUE* (filled circles) and *Voyager* fluxes (open circles) from Holberg (1985) for BD +28°4211. The *IUE* data are the average of 12 large- and 12 small-aperture spectra in 5 Å bins. Typical error bars due to counting statistics are shown for *Voyager*, while the *IUE* error bars represent the expected error in the average spectrum. Some spectral absorption lines are identified.

FIG. 4.—Same as Fig. 3, for BD +75°325. *IUE* data are from seven large- and six small-aperture spectra.

1σ *Voyager* statistical uncertainty, the *Voyager* points for BD +75°325 lie systematically above the *IUE* data by $\sim 15\%$. This minor discrepancy is unexpected, since *Voyager* is calibrated to the *IUE* scale in the region of overlap. The small statistical error bars for BD +28°4211 are independently verified by the quantitative agreement between the weak low-dispersion features near 1340 and 1370 Å in Figure 3 and the same features identified in high dispersion by Schönberner and Drilling (1985) and Dean and Bruhweiler (1985).

Despite the small disagreement between *IUE* and *Voyager* for BD +75°325, the *Voyager* spectrophotometry is probably the most homogeneous data available for calibrating the high-resolution spectrograph on the Hubble Space Telescope (HST) from 1050 to 1150 Å. Holberg *et al.* (1985, and references therein) suggest that the agreement between most *Voyager* data and *IUE* is similar to the case of BD +28°4211 in Figure 3. Independent absolute flux measurements by Woods, Feldman, and Bruner (1985) agree well with *Voyager* fluxes between 1050 and 1150 Å, but the two sets of data do show $\pm 20\%$ variation in their ratios over the same wavelength range. A moderately conservative conclusion is that *Voyager* data have a photometric uncertainty of $\sim 15\%$ for relative fluxes of stars in the region 1050–1150 Å, unless comprehensive evidence is presented to the contrary. However, see Polidan, Carone, and Campbell (1985).

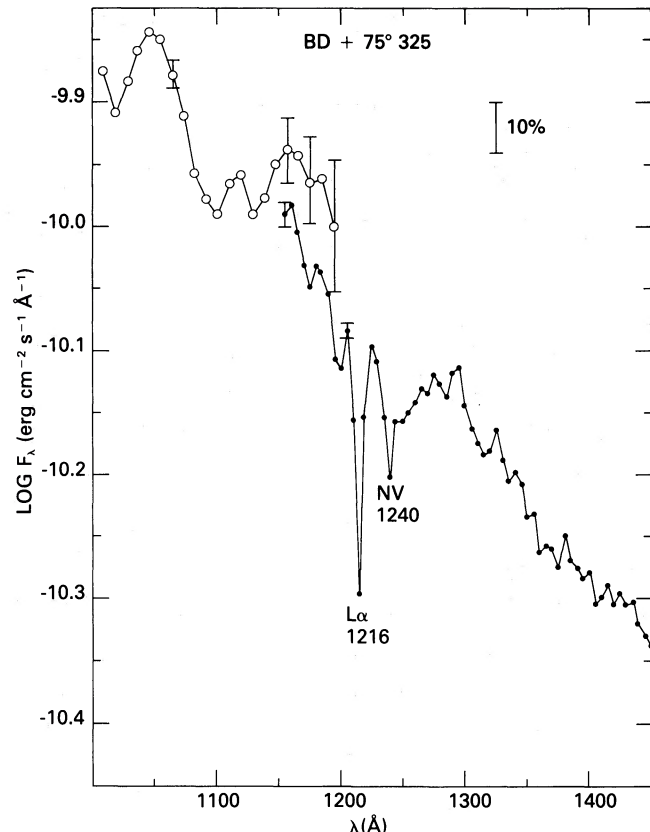


FIG. 4

VI. FUTURE ULTRAVIOLET CALIBRATIONS

Despite the several possible errors at the 1% level outlined here, and despite the potential improvements to the original transfer of the chosen fluxes for η UMa to *IUE* as detailed in Bohlin and Holm (1984), my recommendation is to base all future UV calibrations on the fluxes of the five fundamental standards of Table 2. The overall error in the transfer of the absolute flux scale to *IUE* is still less than the nominal 10% uncertainty in the η UMa fluxes quoted by Bohlin *et al.* (1980).

Specifically, the five *IUE* standards should be the basis for calibration of the LWP camera, for any recalibrations of the SWP and LWR cameras, and for the UV calibration of the HST instruments. The *IUE* observing program that provided the bulk of a larger grid of standards for HST tied these new secondary standards directly to the primary set by observing at least two of the five during each observing run.

New observations by instruments precisely calibrated with respect to the National Bureau of Standards absolute scale are needed. Preference for new observations should be given to the five standards of Table 2. If these stars are too faint, η UMa is the best bright star, because Bohlin *et al.* (1980) based the *IUE* calibration on the choice of flux for this star and because OAO 2 observation showed no UV variability (Holm 1985). Even though exposure times are uncertain when η UMa is rapidly trailed through the *IUE* slit, the shape of the *IUE* flux

distribution can be directly compared with new fundamental observations.

An independent technique for studying the *IUE* calibration error is to compare unreddened sources with physical predictions of their flux distribution, as normalized at $V = 5480 \text{ \AA}$. Especially useful for this purpose are stars with few features, such as hot white dwarfs or main-sequence stars near spectral type B3. If different physical theories all predict the same error for the *IUE* absolute fluxes, this correction could be justified

and would have the virtue of not only eliminating the 10% uncertainty in the chosen flux for η UMa, but also of removing the 2%-4% transfer uncertainty.

Drs. A. V. Holm and J. Koornneef provided valuable constructive criticisms that have been incorporated into this paper. I thank the staff at the Goddard Space Flight Center, who made the data available and are always ready to cheerfully discuss any technical detail of *IUE* data.

REFERENCES

- Bohlin, R. C. 1985, *NASA IUE Newsletter*, **26**, 20.
 Bohlin, R. C., and Holm, A. V. 1980, *NASA IUE Newsletter*, **10**, 37 (=1981, *ESA IUE Newsletter*, **11**, 18).
 ———. 1984, *NASA IUE Newsletter*, **24**, 74 (=1984, *ESA IUE Newsletter*, **20**, 22).
 Bohlin, R. C., Holm, A. V., Savage, B. D., Snijders, M. A. J., and Sparks, W. M. 1980, *Astr. Ap.*, **85**, 1.
 Dean, C. A., and Bruhwiler, F. C. 1985, *Ap. J. Suppl.*, **57**, 133.
 Goy, G. 1973, *Astr. Ap. Suppl.*, **12**, 277.
 Guetter, H. H. 1974, *Pub. A.S.P.*, **86**, 795.
 Harvel, C. A., Turnrose, B. E., and Bohlin, R. C. 1979, *NASA IUE Newsletter*, **5**.
 Hayes, D. S., and Latham, D. W. 1975, *Ap. J.*, **197**, 593.
 Holberg, J. B. 1985, private communication.
 Holberg, J. B., Forester, W. T., Shemansky, D. E., and Barry, D. C. 1982, *Ap. J.*, **257**, 656.
 Holberg, J. B., Wesemael, F., Wegner, G., and Bruhwiler, F. C. 1985, *Ap. J.*, **293**, 294.
 Holm, A. V. 1981, *NASA IUE Newsletter*, **15**, 70.
 ———. 1985, private communication.
 Holm, A., Bohlin, R. C., Cassatella, A., Ponz, D. P., and Shiffer, F. H. 1982, *Astr. Ap.*, **112**, 341.
 Jamar, C., Macau-Hercot, D., Monfils, A., Thompson, G. I., Houziaux, L., and Wilson, R. 1976, *Ultraviolet Bright-Star Spectrophotometric Catalogue* (ESA SR-27).
 Jaschek, C., Hernandez, E., Sierra, A., and Gerhardt, A. 1972, *Catalogue of Stars Observed Photoelectrically* (Univ. of La Plata, Argentina, Serie Astronomica, Vol. **38**).
 Oliversen, N. A. 1983, *NASA IUE Newsletter*, **23**, 31.
 Panek, R. J. 1982, *NASA IUE Newsletter*, **18**, 68.
 Polidan, R. S., Carone, T. E., and Campbell, C. 1985, *Bull. AAS*, **17**, 554.
 Schiffer, F. H. 1980, *NASA IUE Newsletter*, **11**, 33.
 ———. 1982, *NASA IUE Newsletter*, **18**, 64.
 Schönberner, D., and Drilling, J. S. 1985, *Ap. J. (Letters)*, **290**, L49.
 Sonneborn, G. 1984, *NASA IUE Newsletter*, **24**, 67.
 Stone, R. P. S. 1977, *Ap. J.*, **218**, 767.
 Turnrose, B. E., Bohlin, R. C., and Harvel, C. 1979, *NASA IUE Newsletter*, **7**, 17.
 Turnrose, B. E., Bohlin, R. C., Holm, A. V., and Harvel, C. 1979, *NASA IUE Newsletter*, **6**, 180.
 Turnrose, B. E., Thompson, R. W., and Gass, J. E. 1984, *NASA IUE Newsletter*, **25**, 40.
 Wesemael, F. 1981, *Ap. J. Suppl.*, **45**, 177.
 Wesemael, F., Auer, L. H., Van Horn, H. M., and Savedoff, M. P. 1980, *Ap. J. Suppl.*, **43**, 159.
 Woods, T. N., Feldman, P. D., and Bruner, G. H. 1985, *Ap. J.*, **292**, 676.

RALPH C. BOHLIN: Space Telescope Science Institute, Homewood Campus, 3700 San Martin Drive, Baltimore, MD 21218